MDPI

Article

Validation of a system to estimate spatio-temporal gait parameters in real time using a LRF sensor, Online estimation of gait spatio-temporal parameters using a LRF sensor

Andres Aguirre [1,†,‡], Carlos A. Cifuentes [1,‡] and Marcela Munera [2,*]

[1] Affiliation 1; e-mail@e-mail.com
[2] Affiliation 2; e-mail@e-mail.com
* Correspondence: e-mail@e-mail.com; Tel.: +x-xxx-xxx-xxxx
† Current address: Affiliation 3
‡ These authors contributed equally to this work.

Academic Editor: name
Version March 17, 2019 submitted to Entropy; Typeset by LaTeX using class file mdpi.cls

Abstract: The real-time estimation of spatio-temporal gait parameters (STGP) is very used for giving feedback during therapies or controlling devices focused in helping gait rehabilitation. The most used sensors for this applications are the wereable sensors (WS), many studies have been carried out with the aim to validate their STGP measurements with a gold standard system. The laser range finder (LRF) is a non wereable sensor (NWS), which have been used in practical applications to estimate STGP and it has demonstrated a great potential. However, the LRF measurements haven't been validated with a gold standard system, therefore the aim of these study is to develop a model to estimate in real-time the STPG using a LRF and validate them with a BTS motion analysis system. The results present that the proposed model doesn't have a significant difference with the gold standard measurements. El abstract debe tener una motivación, objetivo de investigacion, etapas desarrolladas, resultados obtenidos y conclusiones mas relevantes

Keywords: Laser range finder; spatio-temporal; gait parameters; real-time estimation; WFLC; FLC

1. Introduction

General spatio-temporal gait parameters (STGP) are used for assessing patients with gait impairments, those parameters are: cadence, stride length and speed [1]. Online estimation of STGP is very useful in some health applications, one of the most common uses is to control robotic rollators to give assistance to patients with gait impairments [2–8]. no se entiende cual es el otro tipo de robots, hay que ser mas claro en las explicaciones This approach is also used to control another kind of robots which assist gait rehabilitation [9] or to give feedback during therapy Explica que tipo de feedback y las aplicaciones [10–12]. hay concluir algo en este parrafo

Many studies have been carried out to propose and assess sensor devices for measuring STGP, this this, cual? en que nosotros proponemos? devices can be classified in two groups, wereable sensors (WS) and non-wereable sensors (NWS) [13]. The NWS are usually based on image processing or floor sensor que es un floor sensor??? debes ser mas preciso en tus comenarios, ya que esto es un artículo cientifico, ejemplo de sensores por imagenes con referencias, those sensors don't don't y ninguna otra contracción no se usa en texto cientifitico = do not need to attach any sensors to the person who is assessed, nevertheless these sensors require a controlled environment for obtaining a proper operation, which limitates their use in real scenarios (outside the laboratory)

[13]. The WS systems attach sensors on specific parts of the body, thus they can be used in several environments and give autonomy to the patient que tipo de autonimia, de nuevo hay que ser claro en las afirmaciones y sustentarlas en referencias, however they can be affected by external factors and have power supply restrictions [13]. There are many kind of sensors that can be classified in this group (force sensors, extensometers, active markers, accelerometers, gyroscopes, etc). However, the most used for gait analysis are the inertial measurement units (IMU) [13–15]. porque que eficiencia tienen, que los hace ser los mas usados???

Force platforms and movement analysis systems based on infrared cameras are considered as the gold standard for measuring STGP, this is because of their high accuracy [16–19], nevertheless they are very expensive and can't be used outside laboratories [13]. Besides, distinguishing load charges generated on the force platforms is not a simple task [20] and the systems movement analysis require a complex and heavy process to detect body parts [13], therefore it is difficult to get online estimation of STGP with these systems.

Many studies have used WS such as: IMUs, pressure sensors and footswitches, to measure STGP in real-time, moreover these studies have compared the measurements of the proposed systems with the measurements gotten with gold standard systems [21–26]. These studies have consisted in evaluating the proposed systems at different types of walk (pathological, slow walk, normal walk and fast walk) and their results have shown that it possible to measure stride length with a an error of 2.3% aqui hablas de los errores y los anteriores no, debes presentar todos los sensore de la misma manera and gait phase events detection with an error of 40ms, however this detection (which is necessary for getting cadence) has shown an error of 20% [26].

These systems have 5 important issues which consist in creating wireless communication to get data, improving real-time processing, miniaturizing sensor, reducing power combustion a que te refieres con combustion and a initial calibration [13,26]. Moreover, it is reported that measurements with an error higher that 10% are not enough for practical applications [26], hence studies have concluded that is necessary to develop new studies focused in improving accuracy and analyzing which is the optimal sensor [26,27].

Another sensor which has been implemented for estimating STGP is the laser range finder (LRF), this is considered as a NWS and uses an infrared sensor (which is rotating) to determinate planar position and objects distance [13,28–30]. Furthermore, the LRF has been used in practical applications and have shown great potential for estimating STGP in real-time [3,4,6,7,11]

The main advantages of this sensor are: it doesn't need to attach external markers, it doesn't need external calibrations and it can be used indoor and outdoor [28]. On the other hand, its main disadvantage is that it is only able to get planar information from the legs at a fixed height, which can give an error to STGP measurements [28].

Despite some studies have used the LRF to estimate STGP, no one has validated their measurements with a gold standard system [3,4,6,7,11,28–30], unlike how it has been done with others systems mentioned previously [21–26]. Hence the aim of this project is to propose a system which uses a LRF to get STGP and validate them with a movement analysis system based on 6 infrared cameras, at different speeds and inclinations.

The general idea of the proposed system is to realize a legs detection, then with the position of both legs, estimate the distance between them, which will be changing over the time (as an sinusoidal signal) while the persons is walking. Therefore, the frequency and amplitude of the principal component of this signal, correspond to the cadence and stride length [4]. Besides, it is possible to estimate the speed gait multiplying the cadence and the step length [31].

To estimate these three important parameters in real-time, two digital adaptable filters were implemented, those are known as Weighted frequency Fourier Linear Combiner (WFLC) and Fourier Linear Combiner, they are able to estimate the Fourier components of a signal and have been used for estimating pathological tremor from a gyroscope [32] and STGP from a LRF [4] (both in real-time). In order to adjust the LRF measurements which have an error caused by external factors like the height

of the LRF from the floor [4,28], a mathematical model was developed according the errors that the LRF measurements presets with the gold standard measurements.

2. Materials and Methods

In order to develop the proposed system and evaluate it, an study with 28 volunteers was carried out, they were asked to walk on a treadmill at four different speeds and two different inclinations, while an LRF Hokuyo URG-04LX-UG01 was used to track legs position and a BTS movement analysis system with 6 infrared cameras was used to estimate the center of mass (COM) of feet. The study set up can be seen in figure 1, where it can be seen the polar origin of the LRF, its location and the global reference system (GRS) of the BTS cameras.

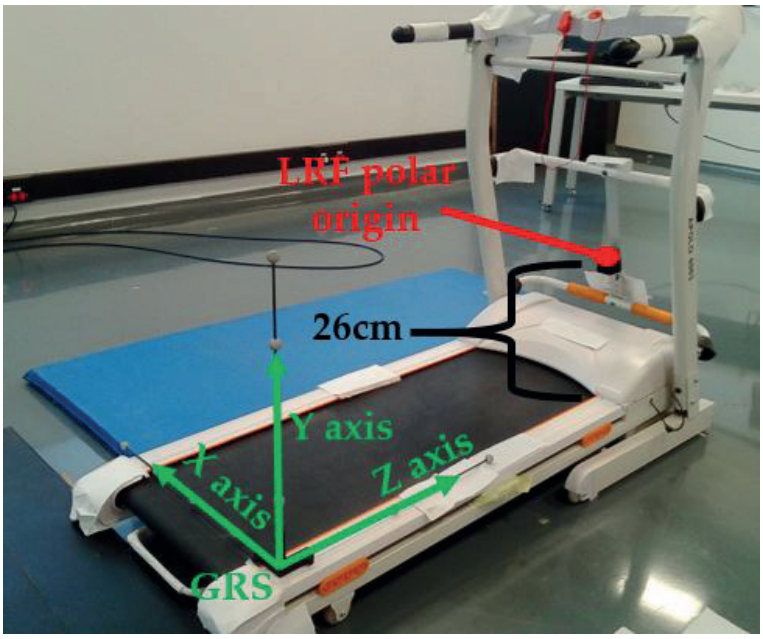

Figure 1. Study's set up, BTS and LRF references on the treadmill

The study was divided in two parts: the fist one, consisted in using the measurements gotten from 18 volunteers to estimate the WFLC and FLC parameters, and estimate the mathematical model to adjust the LRF measurements. The second part consisted in evaluating the proposed model with 10 volunteers, comparing the STGP estimated by the LRF system and the gold standard.

2.1. Subjects

Two groups of volunteers participated in this study, the first group was conformed by 9 females and 9 males, and the second was conformed by 5 males and 5 females. The describing data of both groups can be seen in table 1.

Table 1. Descriptive statics of the groups of volunteers (mean $\pm$ standard deviation)

Group number	Age (years)	Weight (Kg)	Height (cm)
1	23.11 ± 2.82	63.60 ± 9.42	166.72 ± 7.17
2	23 ± 4.83	65.66 ± 7.77	168.20 ± 9.36

The inclusion criteria were that the subjects had to be adults without any difficulty at the moment of walking or physical problems caused by a muscular deterioration associated with the

age. Moreover the subject couldn't have cognitively dispairements preventing them to understand the protocol and the have accepted voluntarily to participate in this experiment.

The exclusion criteria were subjects that had history of injury or surgery on the extremities or on the trunk. Subjects with history of dysfunction in walk, post stroke, muscle-skeletal pathology, cardiovascular limitation and/or neurological diseases. Besides subjects that wear a prosthetic or a orthoses on their lower limbs.

2.2. Protocol

Each subject was asked to walk eight times on the treadmill: The fist four tests consisted in walking 40 steps (approximately) with a speed of 1Km/h, 1.8Km/h, 2.7Km/h and 3.6Km/h without inclination and the last 4 tests consisted in walk on the treadmill at the same speeds with the max treadmill inclination (approximately 3.7^o degrees).

The test started with the location of 14 reflective markers, 5 in each leg and 4 on the treadmill corners. The markers were attached according to the "Davis Heel protocol" and only the markers which are necessary to estimate the feet COM were used [33]. These markers were located on the external head of the fibula, on the external malleus boss, on the calf (with an elastic band and a long bar), on the heel and on the fifth metatarsal boss, it can be seen in figure 2.

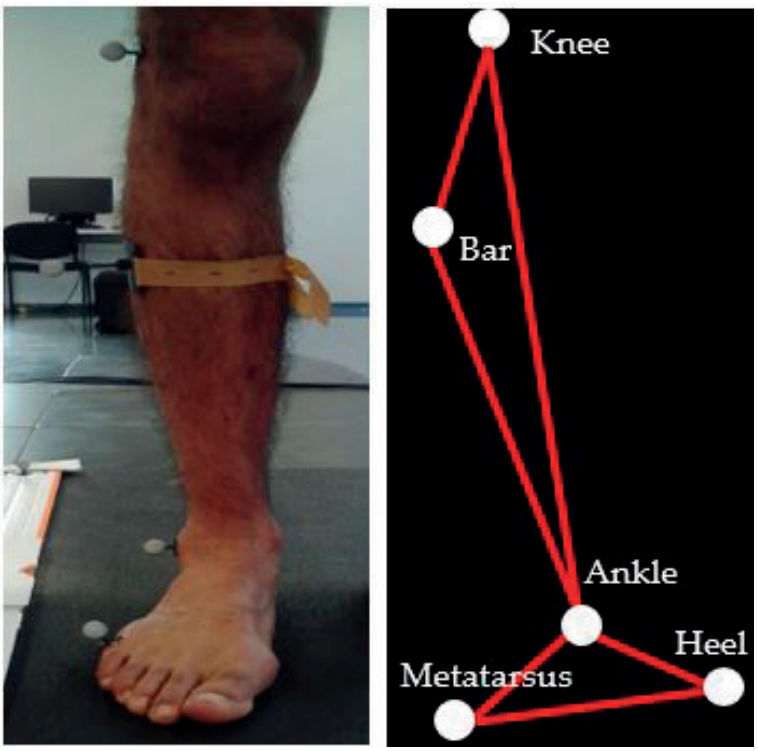

Figure 2. markers location, A markers localization on the right leg, B Markers representation in the BTS software

After the eight testes, the markers were removed form the volunteer and 4 anthropocentric measures on the subject's lower limbs were done, these measures were: the knee diameter and the distance between the lateral malleus to the external malleus (of both legs), these parameters are required to estimate the feet COM [33].

2.3. Laser Range Finder

The LRF implemented was a Hokuyo URG-04LX-UG01, it can be seen in figure 3. It is able to measure distances between 2cm to 560cm with an accuracy of $\pm$3cm, in a range of 240^o with a

resolution of 0.352^o and with a sample rate of 10Hz [34]. It was read by a serial port with a PC and the data were given in polar coordinates, the polar axis origin can be seen in 3.

Figure 3. Hokuyo URG-04LX-UG01 [34]

The sensor was located in front of volunteers with a height of 26cm avobe the treadmill band, it was supported by a metallic bars attached to the treadmill structure (figure 3), which allowed it to remain parallel to the treadmill band, which is important to measure STGP with a LRF [28].

In order to track legs position, the measurement area of the LRF was restricted to the treadmill band area, between 45^o to 135^o and 100mm to 1500mm. Besides, it was assumed that only legs can be in work area, therefore it was possible to estimate legs position detecting the high distance changes in one LRF scan, this method has been used in [4,8] where those high changes are called transition. Figure 4 shown an example of one LRF scan, where Pr and Pl are the right leg and left leg position in polar coordinates, moreover there is also shown the leg difference distance (LDD). .

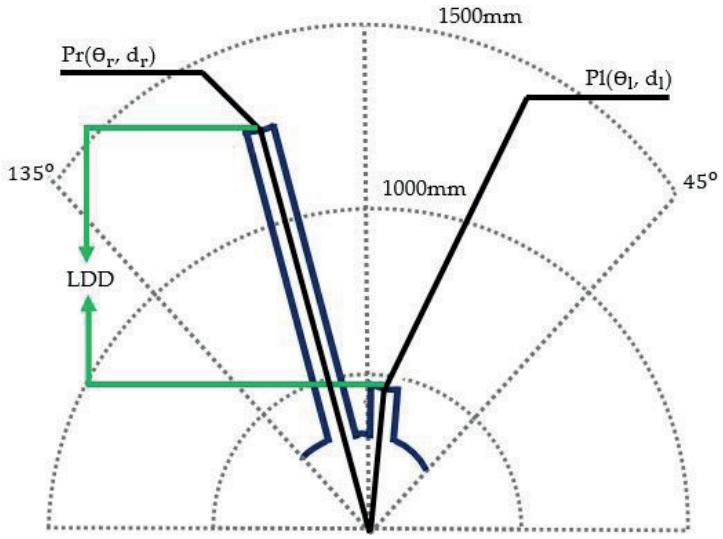

Figure 4. LRF scan and legs detection

In this study it was assumed that a transition higher than 100cm was a transition generated by a leg lecture. In a controlled environment, there are just 2 cases for detecting legs: the first case (figure 5A) is when the legs are enough separated and the scan lecture presents 4 transitions, the second case (figure 5B) is when one leg cover part of the other and the scan present just 3 transitions. Hence the mid points between transitions were taken as the legs position [4,8].

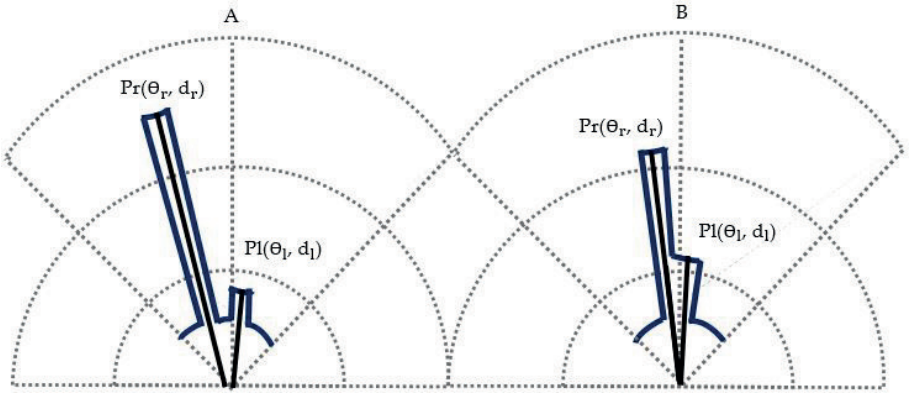

Figure 5. LRF legs position estimation, A when legs are enough separated, B when one leg is covering part of the other leg

According to figure 3, the LDD can be estimated as is shown in equation 1, where "d" represents the distance of the corresponding leg from the polar origin and "θ" the angle of the corresponding leg form the polar axis.

$$LDD = d_l * sin(\theta_l) - d_r * sin(\theta_r) \tag{1}$$

The LDD represent the leg distance on the walk direction, this distance changes as a sinusoidal signal while the subject is walking, it takes positive values when the left leg is back the right leg and it takes negative values when the opposite happens. Each cycle of this LDD signal corresponds to a stride cycle (one step with the right leg and one step with the left one), thus the inverted value of one cycle period, represents the cadence in strides per second [4]. The max value (MV) of each cycle represent the corresponding step length, however this measurement estimated with the LRF is affected by external parameters [4,28]. An example of the LDD signal taken with the LRF can be seen in figure 6

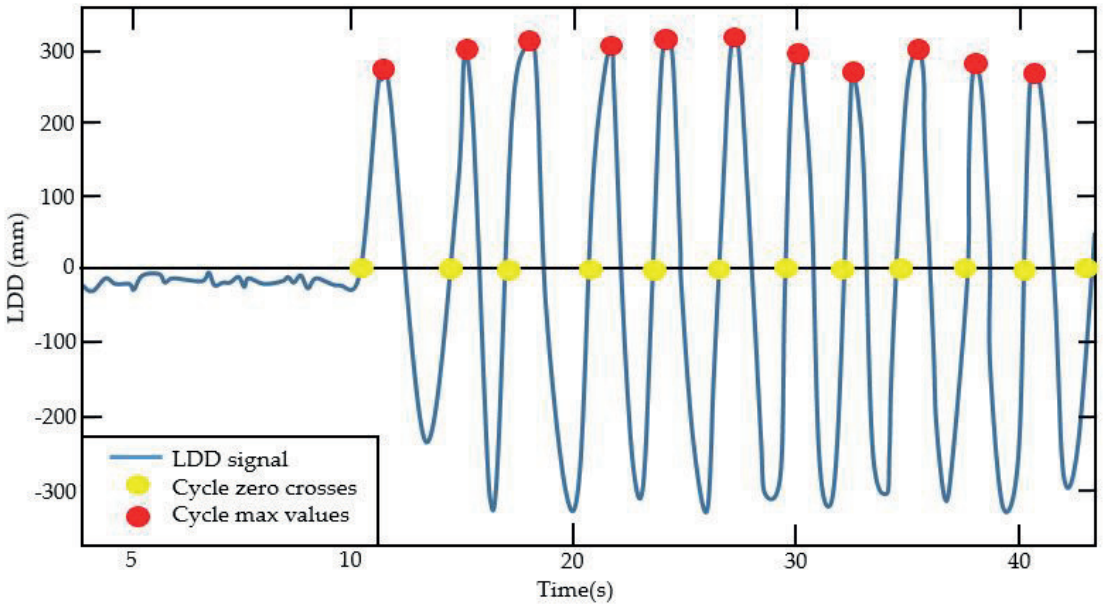

Figure 6. LDD estimated by the LRF while the subject is walking on the treadmill

The cycle time duration can be estimated detecting the zero crosses, with a simple algorithm which determines when the signal changes to negative to positive value, as it is shown in figure

6. However, this method is very susceptible to noises and it would be a problem in a real-time estimation, besides, detecting the MV of each cycle presents the same issue. Therefore, two adaptive filters were implemented to estimate the frequency and the amplitude of the principal Fourier component of each cycle.

2.4. Weighted Frequency Fourier Linear Combiner

The Weighted Frequency Fourier Linear Combiner (WFLC) has been used in tremor modeling [32], it is able to estimate the frequency, the amplitude and the phase of the Fourier components from a signal in real time [35]. The WFCL uses the Least mean square algorithm (LMS) to reduce the error between the real signal and the estimated signal conformed by the Fourier components, it's equations can be seen in equations 2, 3, 4, 5.

$$x_{rk} = \begin{cases} sin(r\sum_{t=1}^{M}\omega_{0_t}), & 1 \leq r \leq M \\ cos(r\sum_{t=1}^{M}\omega_{0_t}), & M+1 \leq r \leq 2M \end{cases} \tag{2}$$

$$\varepsilon_k = S_k - \mu_b - \mathbf{W_k^T X_k} \tag{3}$$

$$\omega_{0_k} + 2\mu_0\varepsilon_k \sum_{r=1}^{M} r(W_{rk}X_{m+rk} - W_{m+rk}X_{rk}) = \omega_{0_{k+1}} \tag{4}$$

$$2\mu_0\varepsilon_k\mathbf{X_k} + \mathbf{W_k} = \mathbf{W_{k+1}} \tag{5}$$

Equation 2 represents the estimation and the Fourier components with an initial ω_{0_t}, equation 3 determined the error between the input signal (S) with the estimated signal conformed by the Fourier components, where $\mathbf{W_k}$ represents a matrix which has the weigh of each Fourier component and $\mathbf{X_k}$ represents a matrix which has each Fourier component value. Equation 4 and 5 show the implementation of the LMS to update the frequency ($\omega_{0_{k+1}}$) and the amplitudes ($\mathbf{W_{k+1}}$).

The WFLC has 4 parameters: M, that is the number of harmonics to estimate the input signal; μ_0, which is a gain used to adapt the frequency estimation; μ_1, which is a gain used to adapt the amplitudes estimation and μ_b, that is used to compensate low frequency errors [32]. Besides, it is required that the input signal oscillates in a range from -1 to 1, therefore it is usually divided by a normalization value (NV) [35].

In this study the LDD signal was divided by 1000 and was used as the input signal of the WFLC, the M parameter was set to 1, because only the principal component is required for estimating the cadence and the step amplitude [4]. The other three parameters were fixed based on the experimental data obtained with the fist group. In order to estimate the right parameters, the frequency and the max values (MVs) of each LDD cycle were extracted for each test without inclination (18 subjects at 4 speed, which means 72 LDD signals and each one with 40 steps approximately) in an off-line process. This process consisted in detecting the zero crosses and the MVs of each cycle, then the WFLC results were simulated and evaluated, the parameters established and initial values can be seen in table 2, moreover an example of a simulation is shown in figure 7.

Table 2. WFLC parameters and initial values)

WFLC parameter	Value
M	1
μ_0	0.15
μ_1	0.4
μ_b	0
ω_0 (initial value)	0.5(Hz)
W (initial value)	[0 0]
NV	1000

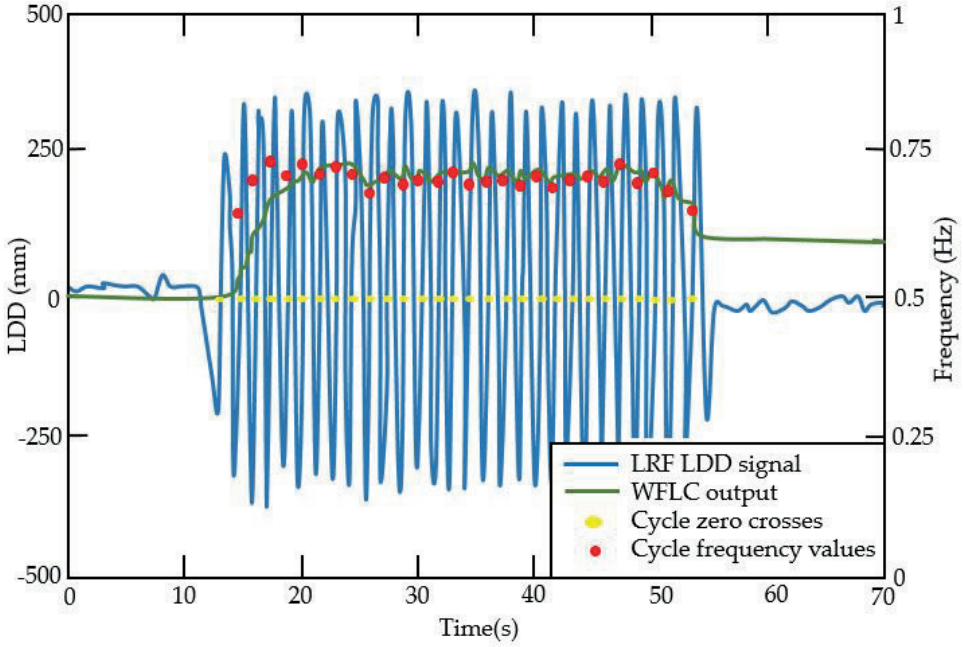

Figure 7. simulation of WFCL frequency estimation, the signals were taken from a test at a speed of 2.7Km/h

The sequence of the WFLC equations is done when a sample of the input signal appears, for this case the LRF sample rate is 10Hz, therefore the WFCL is updating the frequency and the harmonic weights every 0.1s. Thus, in figure 7 the WFLC frequency estimation looks like a signal.

2.5. Fourier Linear Combiner

The Fourier Linear Combiner (FLC) is simpler that the WFCL, it only estimates the amplitudes of the Fourier components, however the FLC needs to know the frequency of the input signal. Despite the WFLC estimates the amplitudes, those can be affected by the frequency estimation,therefore it is better to estimate them with the FLC [4]. It also requires that the input signal (Y) is normalized and the signal frequency (ω_0) is now an input. Furthermore, it has two parameters: M, which es the number of harmonics to estimate the input signal and μ, which is used as a gain for estimating the harmonics weights (equation 8), equations 6, 7 and 8 show the FLC operation [36].

$$x_{rk} = \begin{cases} sin(r\omega_{0_k}), & 1 \leq r \leq M \\ cos((r-M)\omega_{0_k}), & M+1 \leq r \leq 2M \end{cases} \tag{6}$$

$$\varepsilon_k = Y_k - \mathbf{W_k^T X_k} \tag{7}$$

$$2\mu\varepsilon_k \mathbf{X_k} + \mathbf{W_k} = \mathbf{W_{k+1}} \tag{8}$$

The ω_{0_k} is estimated with the WFLC, the **W** and **X** matrices correspond to the weighs and values of the Fourier components, the estimate amplitude of Y is the magnitude of **W** multiplied by the NV [36]. With the data of the fist group of volunteers, the parameters of the FLC were set in: 1 for M, 0.2 for μ, 1000 for the NV and [0 0] as the initial value of **W**. Similar to the WFLC, the peaks of each cycle were detected in an off-line process, then these values were used to evaluate the FLC amplitude estimation, an example of this can be seen in figure 8. Just as it happens in the WFLC, the FLC updates the harmonic weights when a sample of the input signal appears (every 0.1s). Thus, in figure 8 the FLC amplitude estimation looks like a signal.

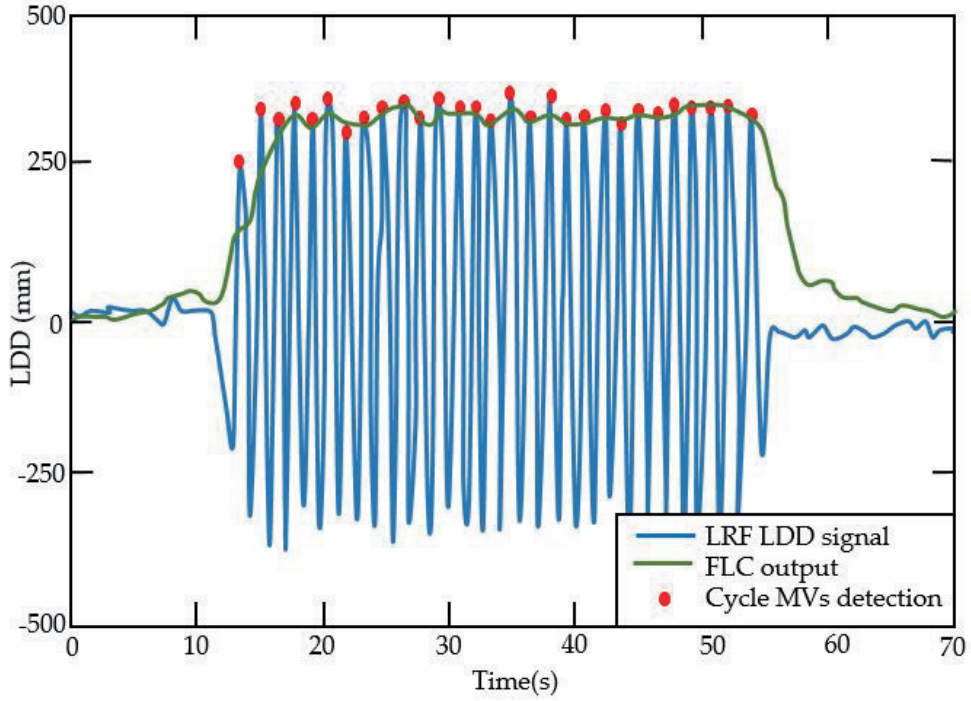

Figure 8. Simulation of FCL amplitude estimation, the signals were taken from a test at a speed of 2.7Km/h

2.6. BTS movement analysis system

A Smart DX motion capture system of the (from the BTS bioengeniering company) with six infrared cameras was used to track the feet COM analysis system, it is able to measure 100 frames per second with an accuracy lower than 0.1mm [37]. In each test, the BTS system was calibrated with an accuracy lower than 0.5mm and with the Z axis of the reference system, in the opposite direction of the treadmill band movement and with no treadmill inclination (figure 1). Besides, 4 reflective markers were located on the treadmill corners to estimate treadmill inclination and the treadmill band direction when the inclination changes.

In order to track the feet COM, 5 reflective markers were attached to each volunteer's legs (figure 2) and 4 anthropometric measures were done according to the "Davis heel protocol" [33]. The basic idea is to use the knee (Km), shank (Sm) and ankle (Am) markers to generate a local reference system (LRS) on the ankle marker, then using the malleus distance, the local system Y axis and the metatarsus marker (Mm) to estimate the ankle center rotation (ACR) and the foot center rotation (FCR), which are the points that represent the foot segment [33]. According to [38] the foot COM is located at the

mid of the foot segment, an example of the ACR, FCR, LRS and the foot COM estimation can be seen in figure 9.

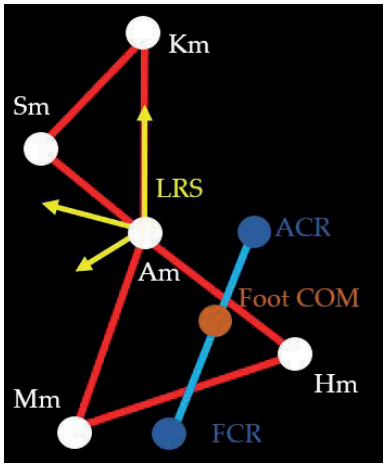

Figure 9. ACR, FCR, reference system and the foot COM estimation

According to figure 1, when there is no inclination the LDD can be estimated as the difference between the z component of the right foot COM and the z component of the left foot COM (it is the opposite order of the LRF because, the reference systems are in opposite direction). Similarly to the LRF LDD estimation, the zero crosses and the MV of each cycle were estimated from the 4 first testes of the fist study group. An example of the LDD signal estimated with the BTS system and the LRF can be seen in figure 10.

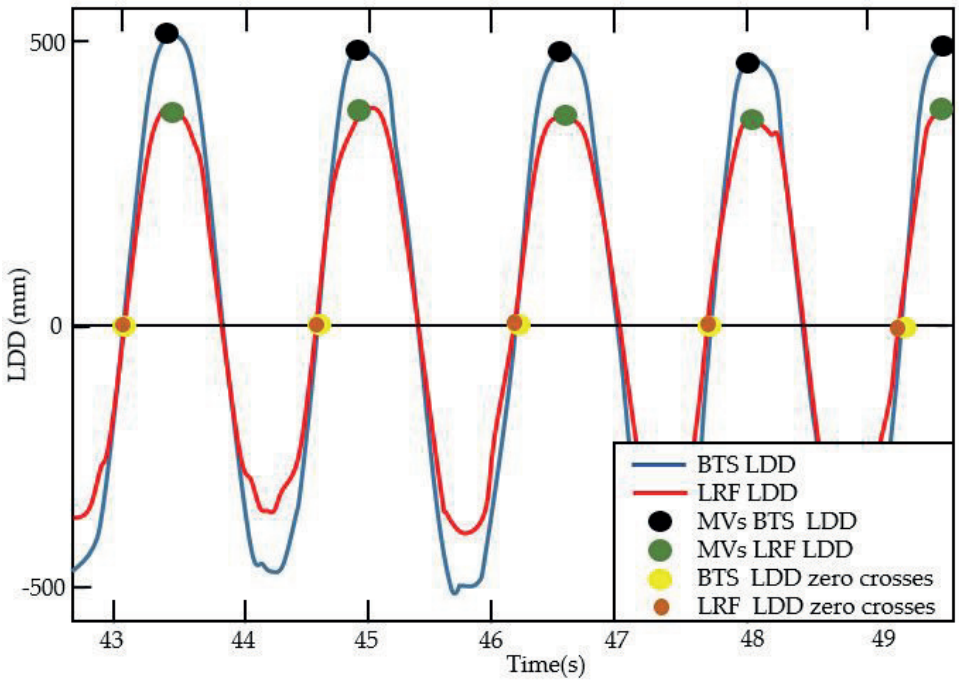

Figure 10. LDD estimated with the BTS system and the LRF

It is possible to see in figure 10, that the zero crosses detection are very similar in both signals, thus the cadence is also similar, nevertheless the LRF MVs are lower than the gold standard. To determinate if there was a significant differences between the LRF and BTS measurements, both parameters (cadence estimated with the zero crosses and MV) of each LDD cycle of the 72 signals

(4 tests without inclination and 18 volunteers) were estimated, then these values were clustered in 8 groups (according to the treadmill speeds and the parameters) and a Wilcoxon test (with a significance level of 5%) was implemented to each group. The descriptive statics of each group and the Wilcoxon results are shown in table 3, furthermore, to determinate if any group had a normal distribution a Shapiro-Wilk test (with significance level of 5%) was applied to each one, however no one showed enough statistical evidence to accept the null hypothesis.

Table 3. Descriptive statics of the parameters gotten with the first group of volunteers and results of the Wilcoxon test (mean $\pm$ standard deviation,* groups which show a significant difference)

Treadmill speed	Parameters	Cameras	LRF	Wilcoxon P value
1 Km/h	Cadence (strides/s)	0.476 ± 0.089	0.474 ± 0.066	0.832
	MV (mm)	286.923 ± 50.828	252.475 ± 40.085	$8.752 * 10^{-5}$*
1.8 Km/h	Cadence (strides/s)	0.564 ± 0.079	0.565 ± 0.149	0.918
	MV (mm)	439.600 ± 49.495	376.458 ± 41.229	$1.3056 * 10^{-7}$*
2.7 Km/h	Cadence (strides/s)	0.713 ± 0.080	0.716 ± 0.118	0.810
	MV (mm)	520.696 ± 40.616	421.095 ± 38.304	$3.8631 * 10^{-10}$*
3.6 Km/h	Cadence (strides/s)	0.807 ± 0.084	0.812 ± 0.099	0.732
	MV (mm)	608.400 ± 40.887	503.311 ± 37.980	$7.3638 * 10^{-14}$*

Table 3 shows that the medians of the MVs estimated with the LRF and the BTS systems present a significant difference at each speed, on the other hand, the medians of the cadences show the opposite. This happens because of the external parameters that affects the LRF measurements [4,28], in order to fix it, a mathematical lineal model was developed for adjusting the LRF MVs measurements, this uses the cadence gotten with the LRF to estimate the error between the LRF MV and the BTS MV.

2.7. LRF max values correction

It can be seen in table 3 that the difference between the BTS MVs and the LRF MVs increases as the LRF cadence increases, besides it is possible to determinate the relation (K) between these two measurements as is shown in equation 9, where n corresponds to the group number (according to the treadmill speed), MV_{BTS} corresponds to the mean value of the max values cycles estimated with the BTS system and MV_{LRF} corresponds to the mean value of the max values cycles estimated with the LRF.

$$K_n = \frac{(MV_{BTS})_n}{(MV_{LRF})_n} \tag{9}$$

The values of K and the BTS MVs and the LRF MVs differences can be seen in table 4. The objective of this K value is to determine a parameter which allows to adjust the LRF MV measurements with the gold standard by multiplying the LRF MV with K. With the aim to determinate if there are a lineal dependence between the LRF cadence and the K values, a lineal regression was estimated with the data of table 4, its graph can be seen in figure 11, its equation can be seen in equation 10 and its R value is shown in equation 11.

Table 4. Mean cadence, K values and difference between the media of the LRF MVs ans BTS MVs at each speed

Treadmill speed	LRF Cadence (strides/s)	K	MV difference
1 Km/h	0.476 ± 0.089	1.136	34.448
1.8 Km/h	0.564 ± 0.079	1.168	63.142
2.7 Km/h	0.646 ± 0.080	1.180	79.601
3.6 Km/h	0.807 ± 0.084	1.195	99.089

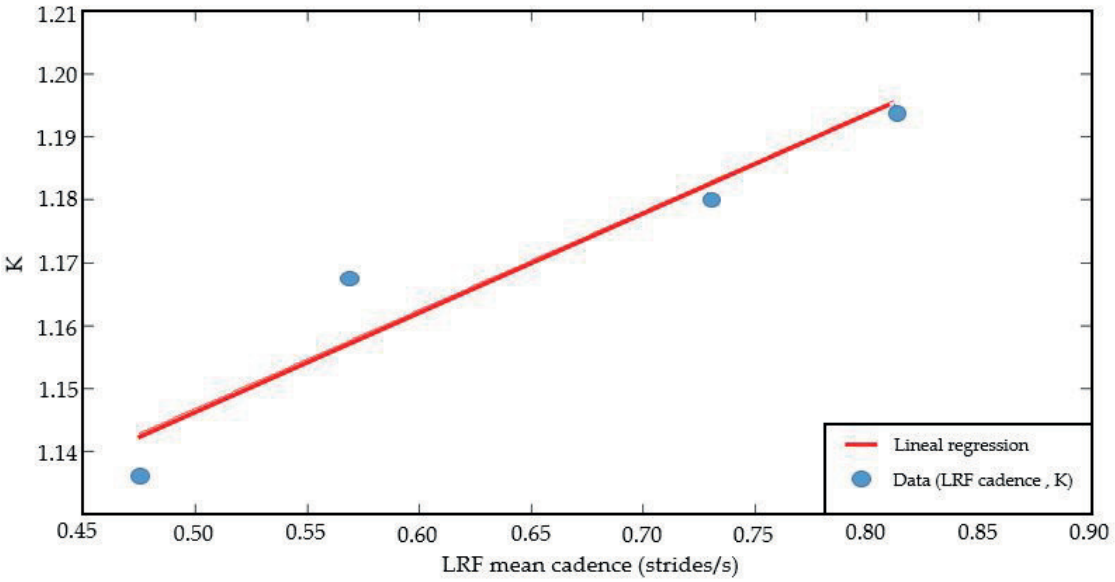

Figure 11. Graph of the lineal regression between K and LRF cadence

$$K = 0.1566(cadence) + 1.0685 \tag{10}$$

$$R = 0.9602 \tag{11}$$

It can be seen in equation 11, that the cadence and the k value presents a strongly lineal relation. In order to assess the performance of the equation 10, the MVs of each cycle (from the 72 signals) were adjusted with a K value, which was estimated with the corresponding cadence cycle and equation 10. Then a Wilcoxon test was done between the BTS MVs and the LRF MVs adjusted, the descriptive statics of each group and the Wilcoxon results are shown in table 5, besides a comparison between the LRF LDD signal and the LRF LDD signal with each cycle adjusted can be seen in figure 12.

Table 5. Descriptive statics of MVs (on the first group of volunteers) estimated with the BTS system and the LRF adjusted with the mathematical linal model, and results of the Wilcoxon test (mean $\pm$ standard deviation)

Treadmill speed	Parameters	Cameras	LRF	Wilcoxon P value
1 Km/h	LRF MV Adjusted (mm)	286.923 ± 50.828	292.246 ± 44.430	0.753
1.8 Km/h	LRF MV Adjusted (mm)	439.600 ± 49.495	444.470 ± 46.570	0.779
2.7 Km/h	LRF MV Adjusted (mm)	520.696 ± 40.616	531.431 ± 44.836	0.511
3.6 Km/h	LRF MV Adjusted (mm)	608.400 ± 40.887	612.848 ± 43.915	0.834

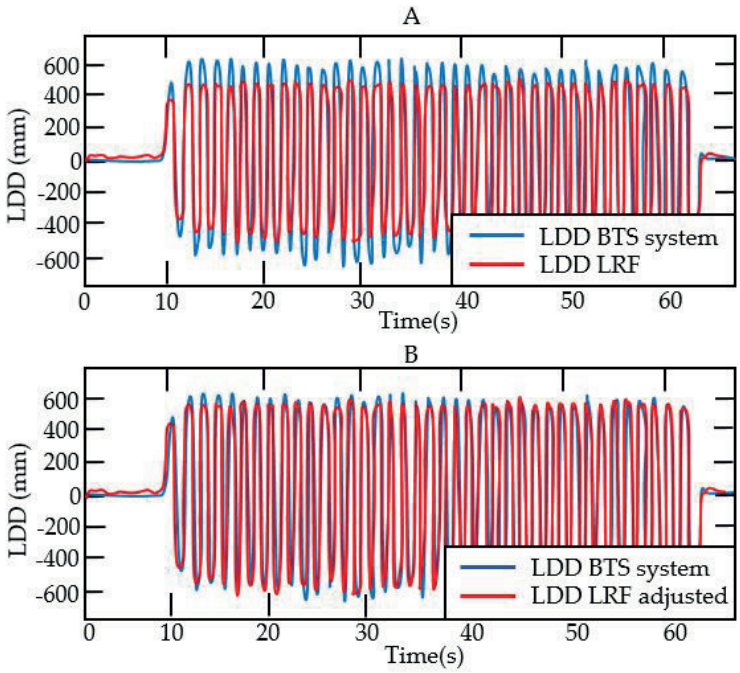

Figure 12. LDD signals without inclination, A LRF signal without adjustment and B LRF signal adjusted, the signals were taken from a test at a speed of 2.7Km/h

It can be seen in table 5 that the difference between the BTS MVs and the LRF MVs have decreased, moreover the medians between any group don't present a significant difference according to the p values. Furthermore, it also shoiws that is possible to use equation 10 and the LRF cadence, which has shown no significant difference with the BTS cadence, to estimate a K parameter for adjusting the MVs of the LDD cycles estimated with the LRF.

2.8. Development of the model to estimate STGP in real-time

According to [4] the principal Fourier component frequency and amplitude, of the LDD signal correspond to the gait cadence and the step length, thus it is possible to estimate the gait speed (GS) multiplying these parameters [31]. However, one LDD cycle is conformed by two steps (right and left step), therefore, if the frequency is estimated in Hz, the cadence is represented in strides/s. Hence, to estimate the gait speed it is necessary to multiply the cadence by 2 and it must be assumed that the right step takes the same time that the left step. This can be seen in equation 12, were CAD is the cadence in strides/s, Sl the stride length in mm and the GS the gait speed in Km/s.

$$GS = 2(CAD)(SL) * 3.6/1000 \tag{12}$$

With the WFLC, the FLC and the mathematical model to adjust the MVs LDD cycles, the model to estimate in real-time the STGP using the LRF was developed. The legs position is the input of the system, then the LDD is estimated and normalized and it is sent to the WFLC and the FLC, the amplitudes estimated by the FLC are adjusted with equation 10 using the cadences estimated by the WFLC, and the GS is calculated with equation 12 using the cadence gotten by the WFLC and the Sl gotten by the FLC adjusted. The diagram of the proposed model (PRMO) can be seen in figure 13.

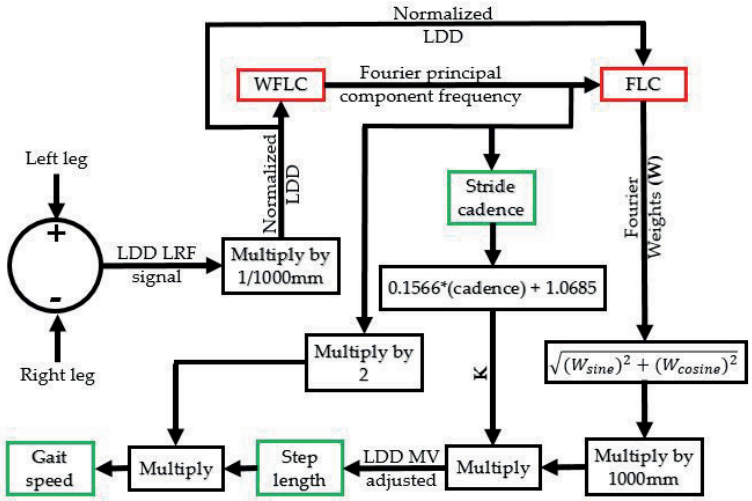

Figure 13. PRMO Diagram to estimate STGP in real time with the LRF

In order to do a initial assessment to the PRMO, an offline simulation was done using the 72 signals of the fist group of volunteers. The PRMO measurements were compared to the MVs and the cadences of each LDD cycle estimated with the BTS system, this comparison was done with a Wilcoxon test. Besides, the root mean square error (RMSE) was estimated for each group, the result of this simulation can be seen in table 6. However, the cadences and MVs estimated by the WFCL and the FLC are updating every 0.1s, while with the BTS systems is needed to get the zero crosses of a whole cycle to estimate those parameters. Hence, in order to compare the BTS parameters with the PRMO measurements, the cadence and MV estimated by the PRMO in the corresponding final sample of a LDD cycle were used for estimating the RMSE and doing the Wilocxon test.

Table 6. Result of the simulation with the PRMO with the LLD signals gotten with the first group of volunteers (mean $\pm$ standard deviation,* groups which show a significant difference)

Treadmill speed	Parameters	Cameras	PRMO	Wilcoxon P value	RMSE
1 Km/h	Cadence (strides/s)	0.476 ± 0.089	$0,492 \pm 0.072$	0.312	0.027
	MV (mm)	286.923 ± 50.828	298.181 ± 40.085	0.510	23.375
1.8 Km/h	Cadence (strides/s)	0.564 ± 0.079	0.571 ± 0.070	0.702	0.012
	MV (mm)	439.600 ± 39.495	431.130 ± 36.244	0.652	19.162
2.7 Km/h	Cadence (strides/s)	0.713 ± 0.080	0.725 ± 0.068	0.530	0.025
	MV (mm)	520.696 ± 40.616	533.707 ± 35.893	0.407	29.212
3.6 Km/h	Cadence (strides/s)	0.807 ± 0.084	0.818 ± 0.077	0.583	0.023
	MV (mm)	608.400 ± 40.887	614.627 ± 31.8652	0.684	17.865

It can be seen in table 6 that neither the cadence nor the MV show a significant difference in their medians at the four evaluated speeds. The highest RMSE cadence is presented in the testes at 1Km/h, which correspond to the 5.672% of the mean gold standard value. The highest RMSE MV is lower than 30mm and it corresponds to the testes at 2.7Km/h, thus this error is equal to the 5.762% of the mean gold standard value. The data of PRMO column can be used to estimate the GS using equation 12, moreover, in order to compare it with the treadmill speed, the units can be changed to Km/h. Table 7 shows the four GS estimations and it is possible to see that the these values are very similar to the treadmill speeds.

Table 7. GS estimated with the mean data of the simulated PRMO measurements

Treadmill speed (Km/h)	GS (Km/h)
1	1.056
1.8	1.772
2.7	2.785
3.6	3.619

2.9. Inclination analysis

In order to estimate the treadmill inclination and how it affects the PRMO measurements acorrding to the BTS system, 4 markers (M1, M2, M3 and M4) were located on the treadmill corners. A vector (Vb) was estimated with the mid point between M1 and M2, and the mid point between M3 and M4 , then Vb was projected on the ZY plane of the global reference system (GRS), this with the aim to estimate the angle (θ) between the Vb projected and the Z axis of the GRS. According to figure 1 the GRS of the BTS system where calibrated with no inclination in the treadmill, therefore the angle represent the treadmill inclination, this process can be sen in figure 14.

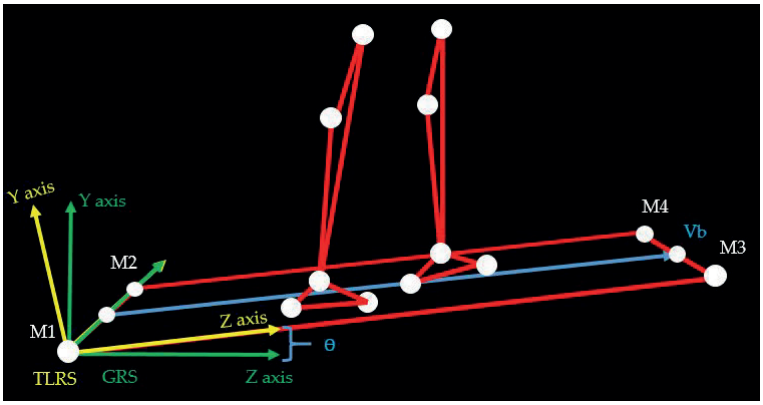

Figure 14. LDD signals without inclination, A LRF signal without adjustment and B LRF signal adjusted

A treadmill local reference system (TLRS) was created by using a normalized vector in the direction of the Vb projected as the Z axis and the perpendicular vector of the plane generated by M1, M2 and M3, as the Y axis. The TLRS was located on M1 and the feet COMs coordinates were transformed to the TLRS, thus the difference between the Z components of the feet COMs represents the LDD. An example of the LDD signal and the estimation of the treadmill inclination during a test can be seen in figure 15.

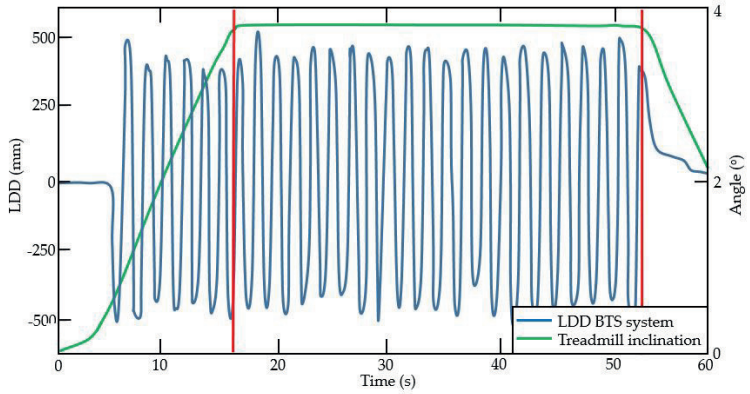

Figure 15. LDD and treadmill inclination with the BTS system, the signals were taken from a test at a speed of 1.8Km/h

It can be seen in figure 15 that the max inclination of the treadmill is approximately 3.7^o, moreover it also shows that the treadmill took a while to reach the max inclination, thus to evaluate how the inclination affects the PRMO measurements, only the LDD cycles that were done during the treadmill max inclination (cycles between the red lines in figure 15) were used for proving the PRMO. In the same way as before, the PRMO measurements were compared using a Wilcoxon test with the gold standard measurements gotten by the BTS system, where the cadence was estimated with the zero crosses detection and the stride length with the MV of each LDD cycle referenced in the TLRS. The result of the Wilcoxon test and the RMSE at each speed can be seen in table 8.

Table 8. Result of the simulation with the PRMO with the LLD signals gotten with the first group of volunteers (mean $\pm$ standard deviation,* groups which show a significant difference)

Treadmill speed	Parameters	Cameras	PRMO	Wilcoxon P value	RMSE
1 Km/h	Cadence (strides/s)	0.448 ± 0.070	0.464 ± 0.066	0.304	0.025
	MV (mm)	330.429 ± 55.134	325.102 ± 49.090	0.747	11.632
1.8 Km/h	Cadence (strides/s)	0.570 ± 0.056	0.579 ± 0.051	0.483	0.006
	MV (mm)	444.578 ± 48.606	435.022 ± 46.274	0.618	22.814
2.7 Km/h	Cadence (strides/s)	0.691 ± 0.062	0.698 ± 0.058	0.655	0.016
	MV (mm)	536.603 ± 42.882	522.621 ± 38.615	0.452	32.905
3.6 Km/h	Cadence (strides/s)	0.801 ± 0.084	0.817 ± 0.075	0.245	0.031
	MV (mm)	613.837 ± 46.449	618.653 ± 43.001	0.788	8.127

Despite the max treadmill inclination was taken into account in the gold standard measurements, table 8 shows that the Wilcoxon test did not determinate a significantly difference between the medians of the PRMO and the BTS system measurements. However, it can be seen that the RMSE values have increased and the P values have decreased for each speed, which shows that the inclination affects the PRMO measurements.

3. Results

In order to evaluate the proposed model in a real situation and with signals that weren't used for developing the PRMO, ten more volunteers were recruited to do the same protocol. However, in this case the STGP were being estimated in real-time by the PRMO, these estimations were saved to compare them with the STGP gotten with the BTS system. Nevertheless, this comparison was done in a post processing, because the STGP in the BTS system can only be estimated in an offline process. As it was done previously, the gold standard cadence was estimated with the zero crosses and the stride length with the MVs of each BTS LDD cycle, this with the aim to see if there are significant differences using a Wilcoxon test and to estimate the RMSE at each speed. The results can be seen in table 9.

Table 9. Comparison results between the STGP estimated by PRMO implemented in real-time and the STGP estimated with the BTS system, using the second group of volunteers (mean ± standard deviation)

Treadmill speed	Parameters	Cameras	PRMO	Wilcoxon P value	RMSE
1 Km/h	Cadence (strides/s)	0.466 ± 0.062	0.454 ± 0.057	0.602	0.023
	MV (mm)	283.104 ± 54.885	290.256 ± 48.435	0.602	18.819
1.8 Km/h	Cadence (strides/s)	0.567 ± 0.051	0.572 ± 0.048	0.788	0.011
	MV (mm)	443.099 ± 35.523	437.991 ± 31.523	0.675	16.739
2.7 Km/h	Cadence (strides/s)	0.677 ± 0.067	0.683 ± 0.061	0.749	0.013
	MV (mm)	549.002 ± 38.066	558.695 ± 34.230	0.540	22.445
3.6 Km/h	Cadence (strides/s)	0.779 ± 0.064	0.789 ± 0.058	0.531	0.018
	MV (mm)	630.283 ± 52.802	637.157 ± 47.242	0.671	18.865

According to the P values that are shown in table 9, no group presents a significant difference between the medians estimated with BTS system and with the PRMO. Besides, no RMSE cadence shows a value higher than 0.023 strides/s, the highest corresponds to the testes at 1Km/h, it means that this error is 4.935% of the mean gold standard value. It can be also seen that no RMSE MV shows a value higher than 23mm, the highest corresponds to the testes at 2.7Km/h, therefore this error is the 4.088% of the mean gold standard value. The GS estimated with the mean data of the PRMO and equation equation 12 can be seen in table 10 .

Table 10. GS estimated with the mean data of the PRMO measurements during the real-time tests

Treadmill speed (Km/h)	GS (Km/h)
1	0.949
1.8	1.803
2.7	2.747
3.6	3.620

An example of the PRMO behavior and a comparison with the gold standard measurements can be seen in figure 16. The blue signal corresponds to the LDD estimated with the BTS cameras system, the brown stars represents the cadence value of each LDD cycle and the red dots are the maximum values of each LDD cycle. The black signal is the cadence estimated by the WFLC, which uses the information from the LRF to estimate the signal frequency, and the green signal is the amplitude estimated by the FLC, that is adjusted by a K value, which is estimated with the cadence obtained with the WFLC and equation 10.

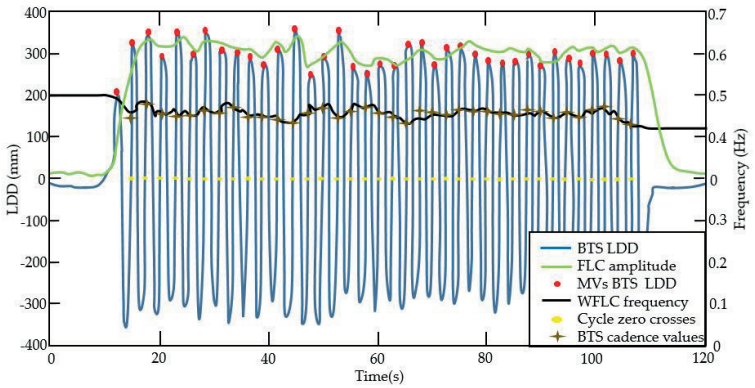

Figure 16. LDD and treadmill inclination with the BTS system, the signals were taken from a test at a speed of 1Km/h

In order to determinate if inclination affects the measurements of the PRMO, the same group of volunteers were asked to walk on the treadmill at the same four speeds with the treadmill maximum inclination. The Results of the testes at the can be seen in table 11.

Table 11. Result of the simulation with the PRMO with the LLD signals gotten with the first group of volunteers (mean ± standard deviation,* groups which show a significant difference)

Treadmill speed	Parameters	Cameras	PRMO	Wilcoxon P value	RMSE
1 Km/h	Cadence (strides/s)	0.451 ± 0.068	0.446 ± 0.059	0.708	0.010
	MV (mm)	343.779 ± 52.657	336.131 ± 46.237	0.717	15.814
1.8 Km/h	Cadence (strides/s)	0.561 ± 0.055	0.574 ± 0.051	0.515	0.019
	MV (mm)	452.062 ± 56.297	441.127 ± 48.341	0.525	26.913
2.7 Km/h	Cadence (strides/s)	0.674 ± 0.048	0.685 ± 0.043	0.632	0.038
	MV (mm)	561.603 ± 37.469	567.785 ± 33.957	0.744	13.706
3.6 Km/h	Cadence (strides/s)	0.762 ± 0.061	0.770 ± 0.054	0.682	0.014
	MV (mm)	652.572 ± 46.854	664.218 ± 41.800	0.462	30.035

4. Discussion

Data in table 9 shows that the signals used for assessing the PRMO (during real time testes) were different to the data that were implemented for developing this model, which are shown in table 6. In general, the cadence of the second group of volunteers is lower than the fist one, and the stride length is higher in the second group. However, results in table 9 show that the PRMO measurements don't present a significant difference compared with the gold standard measurements, besides the cadence and the stride length estimation presents an RMSE lower than 5% in the real time testes.

Table 10 shows that the GS estimated with the means values of the PRMO are very close to the treadmill speed and the simulation results presented in table 7, show that even if the cadence and the amplitude change at the same speed, the GS estimation doesn't change significantly. Hence, the cadence and step length estimated by the PRMO can be used to estimate the gait speed.

Although the treadmill max inclination was set in the last testes, the results in table 11 show that the cadence and the stride length estimated by the PRMO don't present a significant difference from the gold standard measurements. The inclination does not affect the zero crosses of the LDD estimated by the LRF, because this event is still happening when the legs are at the same distance from the LRF, thus, the cadence is not affected. On the other hand, the max values of the LRF LDD is affected by the inclination, due to the LDD is now projected on a different plane. However this projection does not strongly affect this measurement, beacuse, the protection plane has an angle of 3.7^o from the LRF measurement plane, it means that the measurements are modified by the cosine of this angle (0.9979 approximately) which is very close to 1. Therefore, futures studies must focus in prove how higher inclinations affects this measurement and how it can be applied to adjust the LRF measurements.

It can be seen in table 9 and 11 that the standard deviation od the PRMO measurements are lower than the gold standard in the four cases. It happens due to the FLC and the WFLC are configured to ease the strong changes in the gait pattern, that is very useful to make a secure control for assistive devices like robotic walkers [4]. However, it makes that those filters take a time to reach the real values, this phenomenon can be seen in figure 8, where the amplitude estimation signal (green signal) takes one LDD cycle to estimate the amplitude of the LDD signal. In figure 7 a similar behavior can be seen for the cadence estimation, where it takes 3 LDD cycles to reach the real value. Thus, it is important to set the optimal parameters to the WFLC and the FLC.

It can be seen in figure 16 that the estimated cadence signal crosses very near to the dots that represent the gold standard cadence measurements. It happens because the WLFC estimates the LDD frequency gotten by the LRF, which since the beginning in table 3, does not present a significant difference to the LDD frequency gotten by the cameras.

On the other hand, the amplitude estimated signal shown in figure 16 does not cross the gold standard measures as well as the cadence estimated signal, this is due of the LRF amplitude estimation required to be adjusted, because it was being affected and was always lower than the cameras LDD in table 3. However, the PRMO has shown to be able to adjust the LRF amplitude estimation, so it is no longer significantly different to the cameras measurements.

Despite the PRMO has shown a great potential to measure STGP in real time according to a systems which is considered a gold stand for gait measurements, it must be kept in mind that the testes were only done on a treadmill and there are studies which have shown that the STGP on a treadmill can be different from an overground gait [39,40]. Therefore future studies must focus in determining how walking on the floor affects the measurements of the PRMO.

5. Conclusions

The proposed model has shown great result for measuring STGP in real time according to a gold standard measurement system, it hasn't shown a significant error and the highest RMSE is not higher than the 5% for candence and stride length. Furthermore, it is a system that can be applied in several practical applications due to it uses an LRF which has been used to estimate STGP in different field. Future works must focus in studying how inclination and the overground walk affects the measurements of the proposed model.

Supplementary Materials: The following are available online at www.mdpi.com/link, Figure S1: title, Table S1: title, Video S1: title.

Acknowledgments: All sources of funding of the study should be disclosed. Please clearly indicate grants that you have received in support of your research work. Clearly state if you received funds for covering the costs to publish in open access.

Author Contributions: For research articles with several authors, a short paragraph specifying their individual contributions must be provided. The following statements should be used "X.X. and Y.Y. conceived and designed the experiments; X.X. performed the experiments; X.X. and Y.Y. analyzed the data; W.W. contributed reagents/materials/analysis tools; Y.Y. wrote the paper." Authorship must be limited to those who have contributed substantially to the work reported.

Conflicts of Interest: Declare conflicts of interest or state "The authors declare no conflict of interest." Authors must identify and declare any personal circumstances or interest that may be perceived as inappropriately influencing the representation or interpretation of reported research results. Any role of the funding sponsors in the design of the study; in the collection, analyses or interpretation of data; in the writing of the manuscript, or in the decision to publish the results must be declared in this section. If there is no role, please state "The founding sponsors had no role in the design of the study; in the collection, analyses, or interpretation of data; in the writing of the manuscript, and in the decision to publish the results".

Abbreviations

The following abbreviations are used in this manuscript:

MDPI: Multidisciplinary Digital Publishing Institute
DOAJ: Directory of open access journals
TLA: Three letter acronym
LD: linear dichroism

Appendix A.

The appendix is an optional section that can contain details and data supplemental to the main text. For example, explanations of experimental details that would disrupt the flow of the main text, but nonetheless remain crucial to understanding and reproducing the research shown; figures of replicates for experiments of which representative data is shown in the main text can be added here if brief, or as Supplementary data. Mathemtaical proofs of results not central to the paper can be added as an appendix.

Appendix B.

All appendix sections must be cited in the main text. In the appendixes, Figures, Tables, etc. should be labeled starting with 'A', e.g., Figure A1, Figure A2, etc.

Bibliography

1. Whittle, M.W. Clinical gait analysis : A review. *Human Movement Science* **1996**, *15*, 369–387.
2. Cifuentes, C.A.; Rodriguez, C.; Frizera, A.; Bastos, T. Sensor Fusion to Control a Robotic Walker Based on Upper-Limbs Reaction Forces and Gait Kinematics. 5th IEEE RAS & EMBS International Conference on Biomedical Robotics and Biomechatronics, 2014, pp. 1098–1103.
3. Cifuentes, C.A.; Frizera, A.; Carelli, R.; Bastos, T. Human-robot interaction based on wearable IMU sensor and laser range finder. *Robotics and Autonomous Systems* **2014**.
4. C. Cifuentes, A.F. *Human-Robot Interaction Strategies for Walker-Assisted Locomotion*; Springer, Cham, 2016.
5. Ballesteros, J.; Urdiales, C.; Martinez, A.B.; Tirado, M. Online estimation of rollator user condition using spatiotemporal gait parameters. International Conference on Intelligent Robots and Systems (IROS), 2016, pp. 3180–3185.
6. Lee, G.; Jung, E.j.; Ohnuma, T.; Chong, N.Y.; Yi, B.j. JAIST Robotic Walker Control Based on a Two-layered Kalman Filter. IEEE International Conference on Robotics and Automation, 2011, pp. 3682–3687.
7. Papageorgiou, X.S.; Chalvatzaki, G.; Tzafestas, C.S.; Maragos, P. Hidden Markov Modeling of Human Pathological Gait using Laser Range Finder for an Assisted Living Intelligent Robotic Walker. IEEE/RSJ International Conference on Intelligent Robots and Systems (IROS), 2015, pp. 6342–6347.
8. Formation, H.r.; Valadão, C.; Caldeira, E.; Bastos-filho, T.; Frizera-neto, A. A New Controller for a Smart Walker Based on. *Sensors* **2016**, *16*.
9. Hayes, S.C.; Richard, C.; Wilcox, J.; Samantha, H.; White, F.; Vanicek, N.; Clive, S.; Richard, C.; Wilcox, J.; Samantha, H.; Hayes, S.C.; Richard, C.; Wilcox, J.; Forbes, H.S.; Vanicek, N. temporal-spatial characteristics of people with spinal cord injuries : A systematic review The effects of robot assisted gait training on temporal-spatial characteristics of people with spinal cord injuries : A systematic review. *The Journal of Spinal Cord Medicine* **2018**, *0*, 1–15.
10. Gelder, L.M.A.V.; Barnes, A.; Wheat, J.S.; Heller, W. The use of biofeedback for gait retraining: A mapping review. *Clinical Biomechanics* **2018**, p. #pagerange#.
11. Lara, J.S.; Casas, J.; Aguirre, A.; Munera, M.; Rincon-roncancio, M.; Irfan, B.; Senft, E.; Belpaeme, T.; Member, C.A.C. Human-Robot Sensor Interface for Cardiac Rehabilitation. International Conference on Rehabilitation Robotics (ICORR), 2017, pp. 1–6.
12. Janeh, O.; Bruder, G.; Steinicke, F.; Gulberti, A.; Poetter-nerger, M. Analyses of Gait Parameters of Younger & Older Adults during (Non-) Isometric Virtual Walking. *IEEE Computer Society* **2017**, *2626*.
13. Muro-de-la herran, A.; Garcia-zapirain, B.; Mendez-zorrilla, A. Gait Analysis Methods: An Overview of Wearable and Non-Wearable Systems, Highlighting Clinical Applications. *Sensors* **2014**, *14*, 3362–3394.
14. Shull, P.B.; Jirattigalachote, W.; Hunt, M.A.; Cutkosky, M.R.; Delp, S.L. Quantified self and human movement: A review on the clinical impact of wearable sensing and feedback for gait analysis and intervention. *Gait & Posture* **2014**, *40*, 11–19.
15. Embryol, R.J.M. Wearable sensors used for human gait analysis. *Romanian Journal of Morphology & Embryology* **2016**, *57*, 373–382.
16. Grucci, D.; Formento, C. Evaluation of a visual method to calculate temporal parameters. IEEE Biennial Congress of Argentina (ARGENCON); IEEE: Buenos Aires, 2016.
17. Connor, C.M.O.; Thorpe, S.K.; Malley, M.J.O.; Vaughan, C.L. Automatic detection of gait events using kinematic data. *ScienceDirect* **2007**, *25*, 469–474.
18. Jr, J.A.Z.; Richards, J.G.; Higginson, J.S. Two simple methods for determining gait events during treadmill and overground walking using kinematic data. *ScienceDirect* **2008**, *27*, 710–714.
19. Hendershot, B.D.; Mahon, C.E.; Pruziner, A.L. A comparison of kinematic-based gait event detection methods in a self-paced treadmill application. *Journal of Biomechanics* **2016**.
20. Pappas, I.P.I.; Popovic, M.R.; Keller, T.; Dietz, V.; Morari, M. A Reliable Gait Phase Detection System. *IEEE TRANSACTIONS ON NEURAL SYSTEMS AND REHABILITATION ENGINEERING* **2001**, *9*, 113–125.

21. Alvarez, J.C.; Lo, A.M.; Rodriguez-urı, J.; Diego, A.; Gonza, R.C. Real-time gait event detection for normal subjects from lower trunk. *Gait & Posture journal* **2010**, *31*, 322–325.
22. Hanlon, M.; Anderson, R. Real-time gait event detection using wearable sensors. *Gait & Posture* **2009**, *30*, 523–527.
23. Bamberg, S.J.M.; Benbasat, A.Y.; Scarborough, D.M.; Krebs, D.E.; Paradiso, J.A.; Member, S. Gait Analysis Using a Shoe-Integrated Wireless Sensor System. *TRANSACTIONS ON INFORMATION TECHNOLOGY IN BIOMEDICINE* **2008**, *12*, 413–423.
24. Spatio-temporal, R.t.E.; Ferrari, A.; Ginis, P.; Hardegger, M.; Casamassima, F.; Rocchi, L.; Chiari, L. A Mobile Kalman-Filter Based Solution for the Gait Parameters. *IEEE TRANSACTIONS ON NEURAL SYSTEMS AND REHABILITATION ENGINEERING* **2016**, *24*, 764–773.
25. Mannini, A.; Genovese, V.; Sabatini, A.M.; Member, S. Online Decoding of Hidden Markov Models for Gait Event Detection Using Foot-Mounted Gyroscopes. *IEEEJOURNAL OF BIOMEDICAL AND HEALTH INFORMATICS* **2014**, *18*, 1122–1130.
26. Rueterbories, J.; Spaich, E.G.; Larsen, B.; Andersen, O.K. Methods for gait event detection and analysis in ambulatory systems. *Medical Engineering and Physics* **2010**, *32*, 545–552.
27. Aminian, B.K.; Najafi, B. Capturing human motion using body-fixed sensors : outdoor measurement and clinical applications. *COMPUTER ANIMATION AND VIRTUAL WORLDS* **2004**, *94*, 79–94.
28. Pallejà, T.; Teixidó, M.; Tresanchez, M.; Palacín, J. Measuring gait using a ground laser range sensor. *Sensors (Basel, Switzerland)* **2009**, *9*, 9133–9146.
29. Teixidó, M.; Pallejà, T.; Tresanchez, M.; Nogués, M.; Palacín, J. Measuring Oscillating Walking Paths with a LIDAR. *Sensors* **2011**, *11*, 5071–5086.
30. R. Phan-Ba, S. Piérard, G. Moonen, M. Van Droogenbroeck, S.B. Detection and Quantification of Efficiency and Quality of Gait Impairment in Multiple Sclerosis through Foot Path Analysis. 28th Congress of the European Committee for Treatment and Research In Multiple Sclerosis, 2012, Vol. 18, p. 110.
31. N. Sekiya, H. Nagasaki, H. Ito, F.T. The invariant relationship between step length and step rate during free walking. Journal of Human Movement Studies. *Journal of Human Movement Studies* **1996**, *30*, 241–257.
32. Data, G. Real-Time Estimation of Pathological Tremor Parameters from Gyroscope Data. *Sensors* **2010**, *10*, 2129–2149.
33. Roy B.Davis, Sylvia Ounpuu, D.R. A gait data collection and reduction technique. *Human Movement Science* **1991**, *10*, 575–587.
34. HOKUYO. Scanning Rangefinder Distance Data Output/URG-04LX-UG01 Product Details | HOKUYO AUTOMATIC CO., LTD.
35. Vincent Bonnet, Claudia Mazzà, John McCamley, A.C. Use of weighted Fourier linear combiner filters to gyroscope sensors data. *JOURNAL OF NEUROENGINEERING AND REHABILITATION* **2013**.
36. Neto, A.F.; Gallego, J.A.; Rocon, E.; Pons, J.L.; Ceres, R. Extraction of user 's navigation commands from upper body force interaction in walker assisted gait. *BioMedical Engineering OnLine* **2010**, pp. 1–16.
37. BTS Bioengineering. SMART-DX | Motion Capture System | BTS Bioengineering.
38. Winter, D.A. *BIOMECHANICS AND MOTOR CONTROL OF HUMAN MOVEMENT*, 4 ed.; Hoboken, N.J., 2009.
39. Alton, F.; Baldey, L.; Caplan, S.; Morrissey, M.C. A kinematic comparison of overground and treadmill walking. *Clinical Biomechanics* **1998**, *13*, 434–440.
40. Stolze, H.; Kuhtz-buschbeck, J.P.; Mondwurf, C.; Boczek-funcke, A.; Jo, K. Gait analysis during treadmill and overground locomotion in children and adults. *Electroencephalography and clinical Neurophysiology* **1997**, *105*, 490–497.

Sample Availability: Samples of the compounds ..... are available from the authors.